

Heterogeneous & Homogeneous & Bio- & Nano-

# CHEMCATCHEM

CATALYSIS

## Accepted Article

**Title:** Hydrodeoxygenation of phenol over zirconia supported catalysts.  
The effect of metal type on reaction mechanism and catalyst deactivation

**Authors:** Camila Abreu Teles, Raimundo Crisostomo Rabelo-Neto,  
Gary Jacobs, Burtron H Davis, Daniel E Resasco, and Fabio  
Bellot Noronha

This manuscript has been accepted after peer review and appears as an Accepted Article online prior to editing, proofing, and formal publication of the final Version of Record (VoR). This work is currently citable by using the Digital Object Identifier (DOI) given below. The VoR will be published online in Early View as soon as possible and may be different to this Accepted Article as a result of editing. Readers should obtain the VoR from the journal website shown below when it is published to ensure accuracy of information. The authors are responsible for the content of this Accepted Article.

**To be cited as:** *ChemCatChem* 10.1002/cctc.201700047

**Link to VoR:** <http://dx.doi.org/10.1002/cctc.201700047>

## FULL PAPER

# Hydrodeoxygenation of phenol over zirconia supported catalysts. The effect of metal type on reaction mechanism and catalyst deactivation

Camila A. Teles<sup>[a],[b]</sup>, Raimundo C. Rabelo-Neto<sup>[b]</sup>, Gary Jacobs<sup>[c]</sup>, Burtron H. Davis<sup>[c]</sup>, Daniel E. Resasco<sup>[d]</sup>, Fábio B. Noronha<sup>\*[a],[b]</sup>

**Abstract:** This work aims at investigating the effect of the type of metal (Pt, Pd, Rh, Ru, Cu, Ni, Co) on the performance of ZrO<sub>2</sub> supported catalysts for the hydrodeoxygenation of phenol in the gas phase at 573 K and 1 atm. Two different reaction pathways take place depending on the type of the metal. For Pt/ZrO<sub>2</sub> and Pd/ZrO<sub>2</sub> catalysts, phenol is mainly tautomerized, followed by hydrogenation of the C=C bond of the tautomer intermediate formed, producing cyclohexanone and cyclohexanol. By contrast, the direct dehydroxylation of phenol followed by hydrogenolysis might also occur over more oxophilic metals such as Rh, Ru, Co and Ni. In addition to the metals, the oxophilic sites of this support represented by Zr<sup>4+</sup> and Zr<sup>3+</sup> cations near the perimeter of the metal particles also increased the selectivity to deoxygenated products. All catalysts significantly deactivated mainly due to the growth of metal particle size and the decrease in the density of oxophilic sites.

## Introduction

The HDO of phenol reaction has been considered a bifunctional mechanism, requiring a metallic site for hydrogenation/dehydrogenation combined with an acid site of the support for dehydration.<sup>[1]</sup> Thus, understanding the contribution of each type of site in the reaction mechanism is essential for the design of appropriate catalysts.

Several catalysts based on Ni, Co, Fe, Cu, Ni-Cu, Pt, Rh, Pd and Ru dispersed on different supports (e.g., Al<sub>2</sub>O<sub>3</sub>, SiO<sub>2</sub>, CeO<sub>2</sub>, ZrO<sub>2</sub>, CeZrO<sub>2</sub>, V<sub>2</sub>O<sub>5</sub>, C, Mg<sub>2</sub>Al<sub>2</sub>O<sub>4</sub>, TiO<sub>2</sub>, HZSM5 and HY) have been

investigated for the HDO reaction of different model molecules.<sup>[2]</sup> In spite of the numerous studies on HDO of phenol, there have been only few studies about the performance of different metals for this reaction under the same conditions.

Mortensen et al.<sup>[2e]</sup> studied the performance of Ru/C, Pd/C and Pt/C catalysts for the HDO of phenol in liquid phase and correlated, using the work of Norskov et al.<sup>[3]</sup> as a basis, the oxophilicity of the metals (Ru > Pd > Pt) with their deoxygenation activity. Moreover, selectivity depended on the metal as well, with cyclohexane favored on Ru, and cyclohexanol mainly produced on Pd and Pt.

Teles et al.<sup>[4]</sup> investigated different metals supported on silica for HDO of phenol in the gas phase and obtained a correlation between the oxophilicity of the metal and deoxygenation activity. Silica supported Pt, Pd, and Rh tended to produce more hydrogenated products such as cyclohexanone and cyclohexanol; on the other hand, Co, Ni, and Ru favored the production of methane as well as C<sub>5</sub>-C<sub>6</sub> hydrocarbons, due to their greater hydrogenolysis activity. From these results, the authors proposed two different reaction pathways to explain the differences in reactivity. With Pt, Pd, and Rh, the keto tautomer of phenol was hydrogenated at the C=C bond to produce cyclohexanone and cyclohexanol. However, direct dehydroxylation of phenol and hydrogenolysis were deemed to occur over the more oxophilic metals (i.e., Ru, Co and Ni).

The type of the support also plays an important role in the activity, selectivity and stability of the catalysts for HDO of phenol. For example, the role of support on Ni catalysts was investigated for liquid phase HDO of phenol by Mortensen et al.<sup>[2e]</sup> Some metal oxide supports investigated included Al<sub>2</sub>O<sub>3</sub>, CeO<sub>2</sub>, MgAl<sub>2</sub>O<sub>4</sub>, SiO<sub>2</sub>, ZrO<sub>2</sub>, as well as binary systems like V<sub>2</sub>O<sub>5</sub>/ZrO<sub>2</sub> and CeO<sub>2</sub>-ZrO<sub>2</sub>. Carbon, which is typically a relatively inactive support, was also examined. Interestingly, ZrO<sub>2</sub> as a support for Ni particles offered the highest selectivity to cyclohexane. Defect sites (e.g., coordinatively unsaturated zirconia cation sites in the oxide surface) were suggested to stabilize the phenoxide ion in interaction with Ni, thus promoting hydrogenation of the aromatic ring. Cyclohexanone formation was favored, which rapidly converted to cyclohexanol and subsequently dehydrated to cyclohexene. Cyclohexene, in turn, was hydrogenated to cyclohexane. We have also studied the effect of the support on

[a] C. A. Teles, R. C. Rabelo-Neto, F. B. Noronha\*, Catalysis Division, National Institute of Technology, Av. Venezuela 82, 20081-312, Rio de Janeiro, RJ 20081-312, Brazil. Email: fabio.bellot@int.gov.br

[b] C. A. Teles, F. B. Noronha, Chemical Engineering Department, Military Institute of Engineering, Praça Gal. Tiburcio 80, 22290-270, Rio de Janeiro, RJ, Brazil

[c] G. Jacobs, B. H. Davis, Center for Applied Energy Research, University of Kentucky, 2540 Research Park Dr., Lexington, KY 40511, USA.

[d] D. E. Resasco, Center for Biomass Refining, School of Chemical, Biological, and Materials Engineering, University of Oklahoma, 100 East Boyd St., Norman, OK 73019, USA.

## FULL PAPER

the mechanism of HDO of phenol in the gas phase over Pd catalysts supported on SiO<sub>2</sub>, Al<sub>2</sub>O<sub>3</sub> and ZrO<sub>2</sub>.<sup>[5]</sup> Selectivity was found to depend heavily upon the type of support. Over Pd/SiO<sub>2</sub> and Pd/Al<sub>2</sub>O<sub>3</sub> catalysts, the formation of cyclohexanone was favored, whereas benzene was promoted over Pd/ZrO<sub>2</sub> catalyst. These selectivity differences were ascribed to the oxophilicity of the support, whereby coordinatively unsaturated cations near the periphery of metal particles played an important role. The oxygen atom of the keto tautomer intermediate of phenol interacted more strongly with the support, a configuration that favors hydrogenation of the carbonyl group by the metal at the metal-support junction. This, in turn, increased the selectivity to benzene once the hydrogenated intermediate was dehydrated. This work aims at investigating the effect of the metal type on the HDO of phenol over supported catalysts. A systematic study was performed by carrying out the HDO of phenol over ZrO<sub>2</sub> supported metals such as Co, Cu, Ni, Pd, Pt, Rh, and Ru. Zirconia was selected as one of the best supports for deoxygenation due to the presence of oxophilic sites. Catalytic testing and diffuse reflectance infrared Fourier transform spectroscopy (DRIFTS) measurements were carried out to investigate the main reaction pathways on the different metals. The mechanism of catalyst deactivation was also studied using a combination of Raman spectroscopy and model reactions.

## Results and Discussion

### Catalyst characterization

Table 1 shows the metal loadings, surface areas, metal dispersion and rates of HDO of phenol for the various samples. The metal loading of the catalysts was close to the nominal values. The surface areas of all samples were quite similar and around 68 – 78 m<sup>2</sup> g<sup>-1</sup>. The metal dispersions of the catalysts varied from 2 to 62% depending on the metal. Table 1 also lists the metal particle size calculated from the dispersion values considering  $d = 1/D$ .

X-ray diffraction patterns for all catalysts are shown in Fig. S1. The diffractograms of all catalysts showed lines characteristic of a mixture of monoclinic (JCPDS 37-1484) and tetragonal zirconia (JCPDS 17-0923). The procedure outlined by Khaodee et al.<sup>[6]</sup> was utilized to estimate the fraction of each crystalline phase, and the results are listed in Table 1. The monoclinic phase is the dominant one, ranging from 82 - 89% for all catalysts. For Pt, Pd, Rh and Ru catalysts, the lines characteristic of the respective metal oxides were not detected, which is likely due to either their superposition with diffraction lines of the zirconia phases or the low metal loading of the samples. The diffractograms of Cu/ZrO<sub>2</sub>, Ni/ZrO<sub>2</sub> and Co/ZrO<sub>2</sub> catalysts also exhibited lines corresponding to CuO, NiO and Co<sub>3</sub>O<sub>4</sub>.

Fig. S2 shows the TPR profiles of zirconia support and catalysts. The Pt/ZrO<sub>2</sub>, Pd/ZrO<sub>2</sub> and Rh/ZrO<sub>2</sub> catalysts showed H<sub>2</sub>-consumption at 441, 351 and 380 K respectively, due to reduction of PtO<sub>2</sub>, PdO and Rh<sub>2</sub>O<sub>3</sub> oxides.<sup>[7]</sup> The Ru/ZrO<sub>2</sub> catalyst exhibited

three reduction peaks at 370, 403 and 428 K, which originates from the reduction of different RuO<sub>x</sub> species.<sup>[8]</sup> The Cu/ZrO<sub>2</sub> catalyst showed two reduction peaks at 423 and 473 K corresponding to the reduction of CuO dispersed species in weaker interaction with the support and crystalline CuO respectively.<sup>[9]</sup> The H<sub>2</sub>-TPR profile of the Ni/ZrO<sub>2</sub> catalyst showed a small peak at 463 K which was attributed to residual nitrate decomposition. The peak centered at about 588 K and the shoulder at 673 K corresponded to the reduction of bulk NiO and species in strong interaction with the support.<sup>[10]</sup> Two peaks were observed in the TPR profile of Co/ZrO<sub>2</sub>, which are due to the two step reduction of cobalt oxide (Co<sub>3</sub>O<sub>4</sub> → CoO → Co).<sup>[11]</sup>

Hydrogen uptakes determined from the TPR profiles are reported in Table 2. Ru/ZrO<sub>2</sub>, Cu/ZrO<sub>2</sub> and Ni/ZrO<sub>2</sub> catalysts showed a complete reduction of the respective metal oxide, whereas Co/ZrO<sub>2</sub> catalyst had a reduction degree of only 40%. Pt/ZrO<sub>2</sub>, Pd/ZrO<sub>2</sub> and Rh/ZrO<sub>2</sub> catalysts exhibited a hydrogen uptake higher than that corresponding to the complete reduction of the supported metal oxide, indicating that zirconia can be partially reduced, consistent with previously reported XANES results.<sup>[12]</sup>

The dehydration of cyclohexanol has been used as a model reaction for the titration of oxophilic sites.<sup>[12,13]</sup> In our work, the results obtained for zirconia supported catalysts are reported in Table 1. The rate of cyclohexanol dehydration followed the order: Pd/ZrO<sub>2</sub> ≈ Rh/ZrO<sub>2</sub> ≈ Pt/ZrO<sub>2</sub> > Ni/ZrO<sub>2</sub> > Ru/ZrO<sub>2</sub> > Co/ZrO<sub>2</sub>. Recently, the number of acid sites of Pd/ZrO<sub>2</sub> catalysts with different morphologies was determined by temperature-programmed desorption of NH<sub>3</sub> (NH<sub>3</sub>-TPD) and the cyclohexanol dehydration reaction. Both techniques revealed that Pd supported over ZrO<sub>2</sub> with tetragonal structure exhibited the highest density of acid sites. Therefore, the result obtained in this work agrees with the fraction of tetragonal phase present in the zirconia support.

## FULL PAPER

**Table 1.** Pd content, specific surface area, calculated Pd dispersion, reaction rate for dehydration of cyclohexanol (DHA) and for HDO of phenol over zirconia supported catalysts.

catalysts	wt% Metal <sup>[a]</sup>	BET (m <sup>2</sup> g <sup>-1</sup> )	Tetragonal phase (%) <sup>[b]</sup>	Rate of DHA <sup>[c]</sup> (μmolg <sup>-1</sup> catmin <sup>-1</sup> )	d <sub>p</sub> (nm)	Metal dispersion <sup>[d]</sup> (%)	Reaction rate <sup>[e]</sup> (mmol g <sup>-1</sup> Me min <sup>-1</sup> )
Pt/ZrO <sub>2</sub>	0.96	72	17	28.8	2.7	37	41.7
Pd/ZrO <sub>2</sub>	0.96	78	18	29.6	2.6	38	28.6
Rh/ZrO <sub>2</sub>	0.91	72	18	29.2	1.6	62	104.4
Ru/ZrO <sub>2</sub>	5.3	71	13	9.2	12.5 (2.4)	8 (41) <sup>[f]</sup>	3.5
Cu/ZrO <sub>2</sub>	4.9	81	12	7.1	-	-	0.0
Ni/ZrO <sub>2</sub>	9.7	68	16	17.2	25	4	4.4
Co/ZrO <sub>2</sub>	9.4	77	10	6.0	50	2	1.0

<sup>[a]</sup> Measured by XRF<sup>[b]</sup> Calculated by using the data from XRD<sup>[c]</sup> Reaction rate for dehydration of cyclohexanol<sup>[d]</sup> Metal dispersion calculated by H<sub>2</sub> chemisorption (Pt, Rh, Ru, Ni, Co) and cyclohexane dehydrogenation reaction (Pd)<sup>[e]</sup> Reaction rate calculated from a phenol conversion of around 10%<sup>[f]</sup> Ru dispersion of 1%Ru/ZrO<sub>2</sub> catalyst**Table 2.** Hydrogen consumption and reduction degree calculated from the TPR profiles

Catalyst	Theoretical H <sub>2</sub> consumption (cm <sup>3</sup> g <sup>-1</sup> )	Experimental H <sub>2</sub> consumption (cm <sup>3</sup> g <sup>-1</sup> )	Reduction degree (%)
Pt/ZrO <sub>2</sub>	2.21	3.15	142
Pd/ZrO <sub>2</sub>	2.02	3.72	184
Rh/ZrO <sub>2</sub>	5.94	7.06	118
Ru/ZrO <sub>2</sub>	32.83	35.24	93
Cu/ZrO <sub>2</sub>	17.27	14.41	100
Ni/ZrO <sub>2</sub>	37.01	34.16	92
Co/ZrO <sub>2</sub>	47.65	19.25	40

**HDO of phenol over Me/ZrO<sub>2</sub> catalysts**

The phenol conversion and product yield as a function of W/F at 573 K over all catalysts are shown in Fig. 1. All catalysts were active for HDO of phenol except Cu/ZrO<sub>2</sub>, which did not display any activity at the highest W/F used. The zirconia support was also tested and was not found to be active under the reaction conditions used. Thus, the catalysis likely occurs on the surface of metal particles and/or at the junction between metal particles and the support. Table 1 lists the deoxygenation reaction rates calculated using the data obtained under differential reaction conditions (i.e., conversion of around 10%). Rh/ZrO<sub>2</sub> catalyst exhibited the highest reaction rate, which followed the order: Rh/ZrO<sub>2</sub> > Pt/ZrO<sub>2</sub> > Pd/ZrO<sub>2</sub> > Ni/ZrO<sub>2</sub> > Ru/ZrO<sub>2</sub> > Co/ZrO<sub>2</sub>. Recently, we studied the effect of metals for HDO of phenol on SiO<sub>2</sub> supported catalysts.<sup>[4]</sup> Silica was used as an inert support that does not exhibit activity for this reaction. The following order of reaction rates (mmol.g<sup>-1</sup>Me.min<sup>-1</sup>) was observed: Rh/SiO<sub>2</sub> (3.7) > Ru/SiO<sub>2</sub> (2.1) > Pd/SiO<sub>2</sub> (1.3) ≈ Pt/SiO<sub>2</sub> (1.0) > Co/SiO<sub>2</sub> (0.6) ~ Ni/SiO<sub>2</sub> (0.5). This reinforces that the HDO of phenol is strongly influenced by the choice of the metal. However, the comparison between the reaction rates for the catalysts supported on silica and zirconia reveals that ZrO<sub>2</sub> changed the activity order reported for SiO<sub>2</sub> supported catalysts. Furthermore, the reaction rates

significantly increased in the presence of zirconia for all catalysts. For instance, the reaction rate for Rh/ZrO<sub>2</sub> was 28-fold higher than that for Rh/SiO<sub>2</sub>. It is important to stress that the zirconia support did not exhibit activity under this reaction conditions. These results are in agreement with our previous work that revealed an important role of the support on the activity of Pd supported catalysts for HDO of phenol.<sup>[5]</sup> These selectivity differences were explained in terms of the oxophilicity of the support, whereby coordinatively unsaturated cations near the perimeter of metal particles participated in the reaction. Therefore, the activity of zirconia supported catalyst involves not only the intrinsic activity of the metal but also the type of the support.

The product distributions were also remarkably different depending on the metal (Fig. 1). For Pt/ZrO<sub>2</sub>, Pd/ZrO<sub>2</sub> and Ni/ZrO<sub>2</sub> catalysts, cyclohexanone (ONE) and benzene were the main products formed at W/F < 0.15 h. Significant yields of benzene were only obtained at higher W/F. Small amounts of cyclohexanol (OL) and C<sub>12</sub> hydrocarbons such as biphenyl and cyclohexylbenzene were also observed on these catalysts. For Ni/ZrO<sub>2</sub> catalyst, a significant formation of CH<sub>4</sub> was also observed. On the other hand, benzene was the dominant product over the entire range of W/F over the Rh/ZrO<sub>2</sub> catalyst, with only small amounts of CH<sub>4</sub> and C<sub>5</sub>-C<sub>6</sub> hydrocarbons (n-hexane, 2-methylbutane, cyclohexene, cyclohexane) being formed. Besides benzene, significant formation of methane and C<sub>5</sub>-C<sub>6</sub> hydrocarbons was also observed for the Ru/ZrO<sub>2</sub> catalyst. For Co/ZrO<sub>2</sub> catalyst, methane, benzene, o-cresol and C<sub>12</sub> hydrocarbons were the products obtained.

In order to compare the remarkable differences in product distribution over all catalysts, the product selectivities obtained at a similar level of conversion (around 10%) are reported in Table 3. Cyclohexanone and cyclohexanol were the main products formed over Pt/ZrO<sub>2</sub> and Pd/ZrO<sub>2</sub> catalysts, with significant formation of benzene. The highest selectivity to benzene was observed for Rh/ZrO<sub>2</sub> catalyst that also produced C<sub>5</sub>-C<sub>6</sub> hydrocarbons and methane. Ru/ZrO<sub>2</sub>, Ni/ZrO<sub>2</sub> and Co/ZrO<sub>2</sub> catalysts show high selectivities to methane, with the Ru catalyst also producing C<sub>5</sub>-C<sub>6</sub> hydrocarbons. Significant formation of o-

## FULL PAPER

resol and small amounts of  $C_{12}$  hydrocarbons were also observed for  $Co/ZrO_2$ . The selectivity to deoxygenated products (benzene, methane and  $C_5$ - $C_6$  hydrocarbons) followed the order:  $Ru/ZrO_2 > Rh/ZrO_2 \gg Ni/ZrO_2 \approx Pd/ZrO_2 > Pt/ZrO_2 \approx Co/ZrO_2$ .

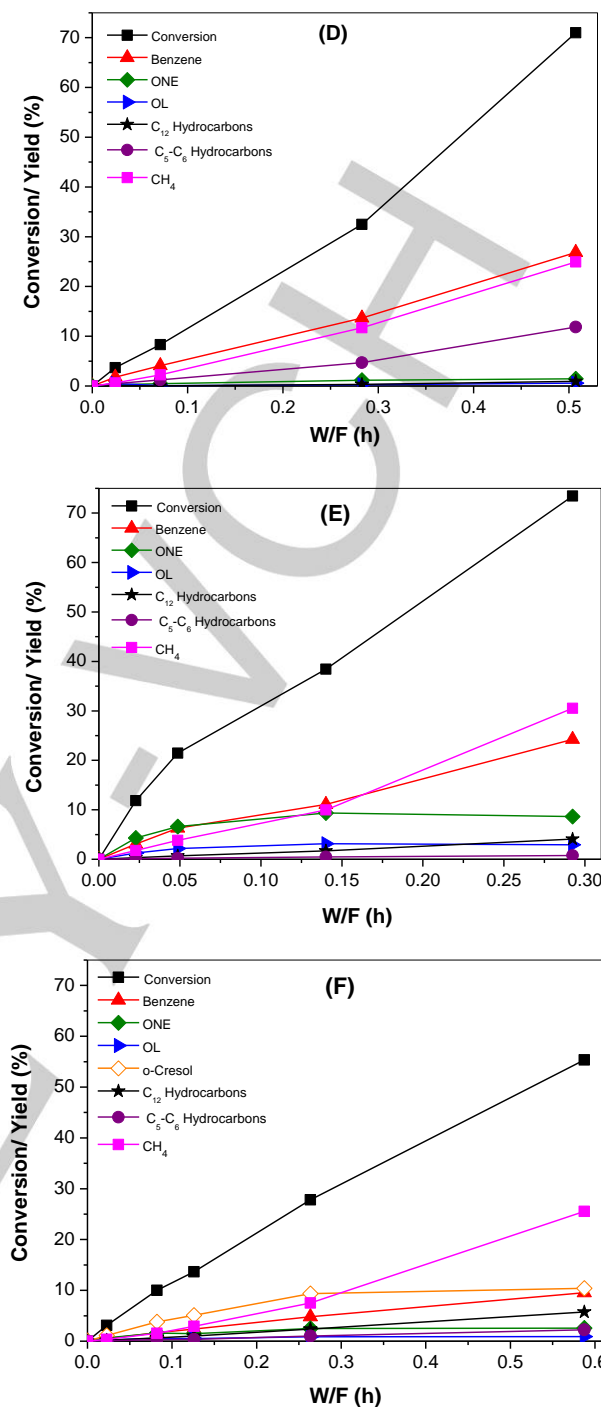
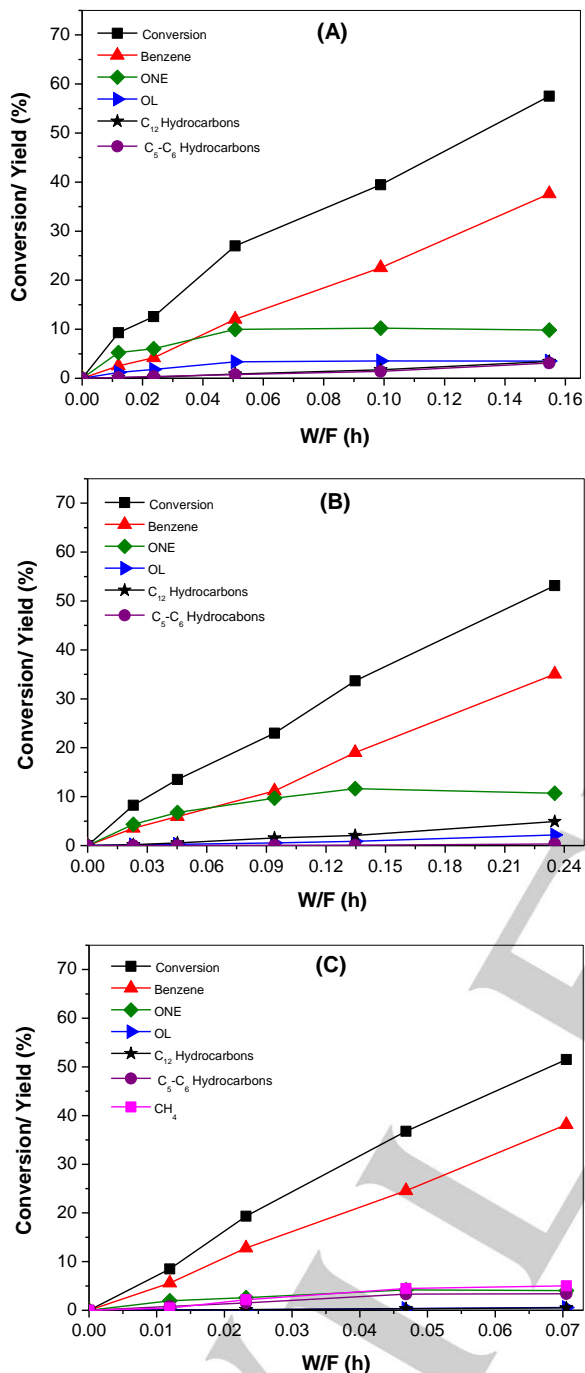


**Figure 1.** Phenol conversion and product yield as a function of W/F over (A)  $Pt/ZrO_2$ , (B)  $Pd/ZrO_2$ , (C)  $Rh/ZrO_2$ , (D)  $Ru/ZrO_2$ , (E)  $Ni/ZrO_2$  and (F)  $Co/ZrO_2$ . Reaction conditions: 573 K, atmospheric pressure,  $H_2$ /phenol molar ratio= 60. ONE: Cyclohexanone; OL: Cyclohexanol.

## FULL PAPER

**Table 3.** Product distributions for HDO of phenol at 573 K and atmospheric pressure over zirconia supported catalysts.

	Pt/ZrO <sub>2</sub>	Pd/ZrO <sub>2</sub>	Rh/ZrO <sub>2</sub>	Ru/ZrO <sub>2</sub>	Ni/ZrO <sub>2</sub>	Co/ZrO <sub>2</sub>
W/F	0.01	0.02	0.01	0.07 (0.15)	0.02	0.08
Conversion (%)	9.3	8.2	8.8	8.3 (12.7)	11.4	10.0
	Selectivity (%)					
ONE	56.6	52.6	22.0	5.6 (6.9) <sup>a</sup>	37.7	16.0
OL	12.8	1.7	--	0.8 (1.7)	10.9	5.7
Benzene	27.4	43.2	63.4	49.7 (74.2)	26.7	16.5
o-cresol	--	--	--	1.1 (-)	5.6	38.0
C <sub>5</sub> -C <sub>6</sub> hydrocarbons	1.8	0.1	9.1	14.9 (8.8)	0.8	3.1
C <sub>12</sub> hydrocarbons	1.4	2.4	0.3	0.6 (-)	2.8	5.4
CH <sub>4</sub>	--	--	5.2	27.3 (8.4)	15.4	15.4

ONE: cyclohexanone; OL: cyclohexanol

C<sub>5</sub>-C<sub>6</sub> hydrocarbons: cyclohexane; cyclohexene; 2-methyl-butane; n-hexane

C<sub>12</sub> hydrocarbons: biphenyl; dibenzofurane; cyclohexylbenzene; pentylbenzene

<sup>a</sup>Selectivities for HDO of phenol over 1%Ru/ZrO<sub>2</sub> catalyst with smaller Ru particle size.

In order to determine the reaction mechanism of HDO of phenol, tests for the conversion of intermediate products (e.g., cyclohexanol and cyclohexanone) over all catalysts and supports under reaction conditions were performed.

#### Cyclohexanol and cyclohexanone conversion over Me/ZrO<sub>2</sub> catalysts

Product yields for each feed at the same conversion level are reported in Table 4. For all catalysts, cyclohexanol was preferentially converted to cyclohexanone, indicating that this reaction is rapid. Pt/ZrO<sub>2</sub>, Ni/ZrO<sub>2</sub> and Co/ZrO<sub>2</sub> catalysts exhibited the highest yields of cyclohexanone. The formation of benzene was quite low for most of the catalysts, suggesting that the reaction of cyclohexanol dehydration is not relevant. Indeed, the cyclohexanol conversion over the zirconia support at the highest W/F (used when feeding phenol over the supported catalysts) was very low, confirming that the contribution of dehydration catalyzed by the zirconia support is negligible. Therefore, benzene cannot be produced by this reaction pathway.

The cyclohexanone was mainly converted to cyclohexanol and bicyclic compounds (typically C<sub>12</sub> hydrocarbons) such as biphenyl, 2-phenylphenol, cyclohexylbenzene, 2-cyclohexylcyclohexan-1-one and 2-cyclohexylphenol. The formation of these bicyclic products has been reported in the literature<sup>[14]</sup> stemming from the alkylation of phenolic and aromatic rings by cyclohexanone. Nimmanwudipong et al.<sup>[15]</sup> observed the formation of C<sub>10</sub>-C<sub>12</sub> hydrocarbons when they studied the conversion of cyclohexanone over Pt/Al<sub>2</sub>O<sub>3</sub> catalysts. Different bicyclic C<sub>12</sub> products were detected by the bimolecular reactions between cyclohexanone and the different products formed during the reaction. This reaction is generally catalyzed by acid sites such as Lewis acid sites. In our work, these reactions could take place

on the Lewis acid sites of the support. Only small amounts of benzene were detected for all catalysts regardless of the metal.

#### DRIFTS experiments of HDO of phenol over zirconia supported

Fig. 2 shows the DRIFTS spectra obtained upon exposure of the zirconia supported catalysts to a phenol/H<sub>2</sub> mixture at different temperatures. At 323 K, adsorption of phenol led to bands characteristic of adsorbed phenoxy species in either the monodentate or bidentate mode<sup>[16]</sup>, including:  $\nu(\text{CH}_{\text{ring}})$  3024-3068 cm<sup>-1</sup>,  $\nu(\text{CC}_{\text{ring}})$  1593-1595 cm<sup>-1</sup>,  $\nu(\text{CC}_{\text{ring}})$  1489-1491 cm<sup>-1</sup>, and  $\nu(\text{CO})$  1292-1294 cm<sup>-1</sup> for monodentate, with a shoulder(s) at 1225-1265 cm<sup>-1</sup> for bidentate. These bands were formed by adsorption of phenol at metal oxide cationic sites. Intensities were highest for the Pt, Pd, and Ni supported catalysts, followed by Rh, and then Ru. Based on the literature<sup>[5]</sup>, bands corresponding to adsorbed cyclohexanol were also observed as follows:  $\nu_{\text{a}}(\text{CH}_2)$  aliphatic CH, 2933-2937 cm<sup>-1</sup>;  $\nu_{\text{s}}(\text{CH}_2)$  stretching, 2856-2860 cm<sup>-1</sup>, CH<sub>2</sub> scissoring, 1452-1454 cm<sup>-1</sup>; CH<sub>2</sub> wagging in the alcohol, 1344-1365 cm<sup>-1</sup>; and  $\nu(\text{CO})$  1070-1167 cm<sup>-1</sup>. These were most significant for the Pt, Rh, and Ru catalysts, followed by the Pd catalyst, with only low intensity bands being observed for Ni. Features between 1620 and 1740 cm<sup>-1</sup> were detected for Pt, Pd, Rh, and Ru catalysts, consistent with  $\nu(\text{C}=\text{O})$  stretching bands, suggesting a small amount of adsorbed cyclohexanone species was also present. Interestingly, the sum of all band intensities was significantly lower for the Ru catalyst, and somewhat lower for Ni as well.

At 373 K, for all catalysts, the relative intensities of the bands corresponding to adsorbed phenoxy species and cyclohexanone decreased while those of cyclohexanol increased. At 473 K, phenoxy and cyclohexanol bands decreased for Pt, Rh, and Ru catalysts, while phenoxy bands continued to decrease and cyclohexanol bands continued to increase for Pd and Ni catalysts. The formation of Pt carbonyl bands was also significant at this temperature. At 573K, all band intensities decreased for Pt, Rh, and Ru catalysts. However, while cyclohexanol band diminished, residual phenoxy bands were still present over Pd and Ni catalysts. At 673 K and 773 K, only traces of bands were present. One exception was Pd, where phenoxy species (albeit at significantly reduced intensity) and a band at 1545 cm<sup>-1</sup> were observed even at 673 K.

The results of DRIFTS are cast in terms of two mechanisms, as supported by prior DFT and experimental investigations: (1) direct dehydroxylation of phenol to a partially unsaturated hydrocarbon surface species (e.g., C<sub>6</sub>H<sub>5</sub>\*), with subsequent hydrogenation to benzene [by analogy with<sup>[17]</sup>], which is favored by metal surfaces such as Ru(0001) or (2) a mechanism involving a keto tautomer intermediate, the latter of which may undergo selective hydrogenation of the carbonyl to 2,4-cyclohexadienone (depending on the support), followed by dehydration to benzene. This was suggested to occur on Pd/ZrO<sub>2</sub> catalysts by experimental observations<sup>[5]</sup>, as well as on Pt (111).<sup>[18]</sup>

## FULL PAPER

**Table 4.** Comparison of performance of catalysts using different feeds: phenol, cyclohexanol (OL) or cyclohexanone (ONE) at 573 K and 1 atm.

	Feed	Conversion (%)	Yield (%)							
			ONE	OL	Benzene	Phenol	o-cresol	CH <sub>4</sub>	C <sub>5</sub> -C <sub>6</sub> hydrocarbons	C <sub>12</sub> hydrocarbons
Pt/ZrO <sub>2</sub>	Phenol	27.1	10.0	3.4	12.0	-	-	-	0.8	0.9
	OL	46.4	42.4	-	0.8	2.5	-	-	0.5	0.2
	ONE	28.4	-	18.2	1.1	4.5	-	-	0.4	4.2
Pd/ZrO <sub>2</sub>	Phenol	23.0	9.7	0.5	11.2	-	-	-	0.0	1.6
	OL	20.8	12.8	-	3.1	3.3	-	-	1.2	0.4
	ONE	15.5	-	3.0	0.1	0.7	-	-	0.1	11.6
Rh/ZrO <sub>2</sub>	Phenol	19.3	2.6	0.1	12.8	-	-	2.2	1.5	0.1
	OL	24.5	15.8	-	4.9	1.5	-	-	2.0	0.3
	ONE	21.8	-	6.1	0.4	1.1	-	-	0.1	14.1
Ru/ZrO <sub>2</sub>	Phenol	32.4	1.1	0.3	14.0	-	0.3	11.7	4.7	0.3
	OL	19.0	16.8	-	0.1	0.5	-	1.0	0.4	0.2
	ONE	22.8	-	5.6	-	-	-	-	-	17.2
Ni/ZrO <sub>2</sub>	Phenol	21.5	4.3	2.2	6.3	-	1.2	4.4	0.2	2.9
	OL	33.3	26.1	-	0.3	6.0	-	0.3	0.1	0.5
	ONE	20.3	-	7.0	0.2	1.1	-	0.5	0.1	11.4
Co/ZrO <sub>2</sub>	Phenol	28.4	2.5	0.9	4.8	-	9.3	7.5	1.0	2.4
	OL	28.5	26.0	-	0.1	1.3	-	0.2	0.6	0.3
	ONE	25.4	-	6.4	-	-	-	-	0.2	18.8

For Ru (0001), an important side reaction was proposed to occur, from prior DFT and experimental work, C-C breaking of the dehydroxylated intermediate, leading to C<sub>1</sub>-C<sub>5</sub> hydrocarbons, consistent with the current reaction testing results (e.g., Figure 3 and Table 3). With Pd and Pt catalysts, and depending on the support utilized, hydrogenation of the 2,4-cyclohexadienone intermediate to cyclohexanone may also occur, with further hydrogenation of the carbonyl to cyclohexanol. This is the reason that oxophilic supports are important for improving selectivity, as preferential adsorption of the keto intermediate by its O atom can facilitate the selective hydrogenation of the carbonyl bond. A screening of metals in Table 3 suggests that Pd and Pt likely follow the second pathway, as selectivities to cyclohexanone (and cyclohexanol, in the case of Pt) side product were higher. Ru had low cyclohexanone and cyclohexanol selectivities, and the highest light side product selectivities, in agreement with the first pathway. The other metals – Rh, Ni, and Co – appear to exhibit aspects of both mechanisms.

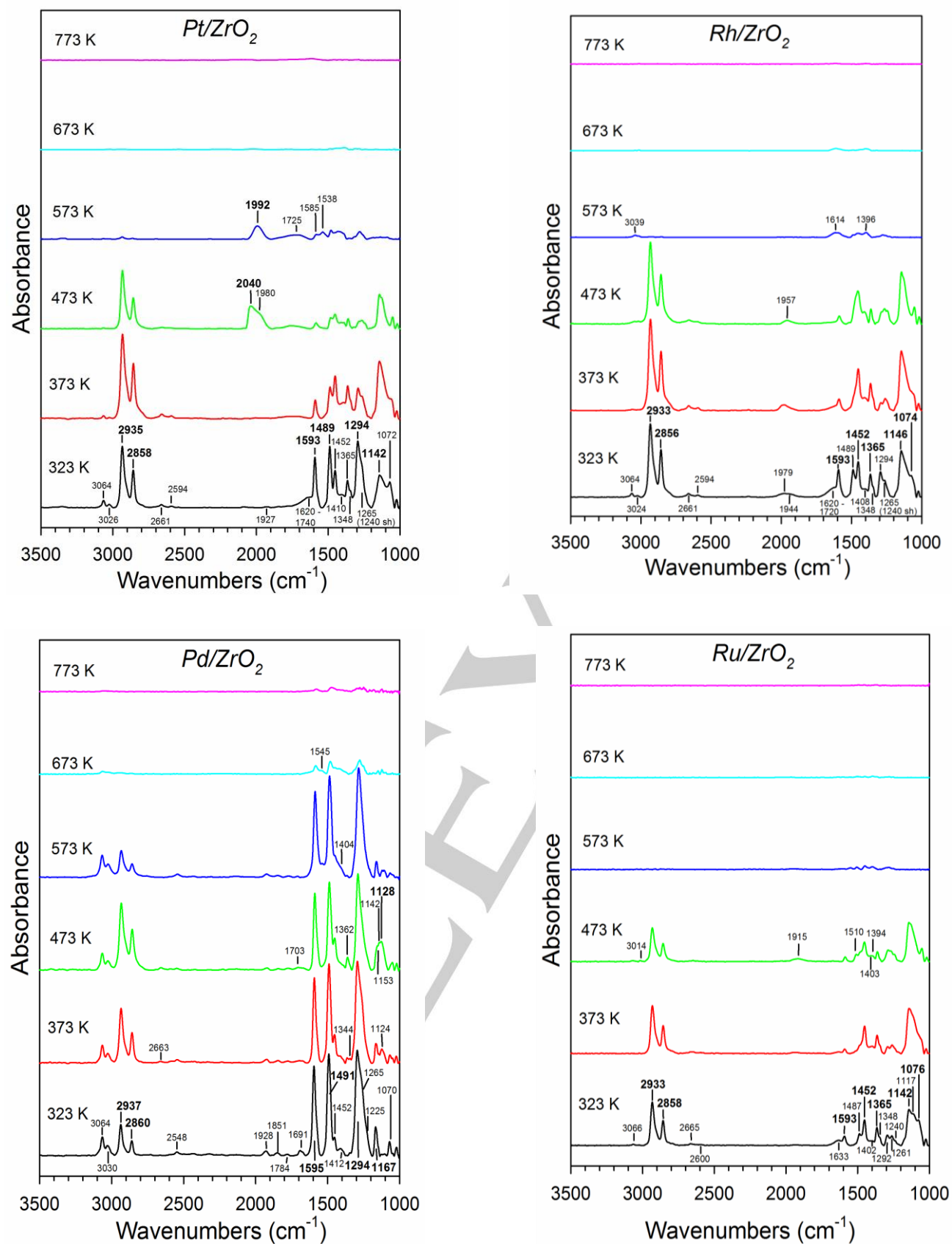
The DRIFTS results lend some support to this. Based on intensity of the bands, the coverage of phenoxy species at 573 K is the highest for Pd, while only traces of bands are detected for Ru. Moreover, although the bands of cyclohexanol were diminished from the 473 K condition, the coverage of cyclohexanol remains significant at least up to 573 K with Pd. In contrast, with Ru, the intensity of cyclohexanol decreases to below detection limits in moving from 473 K to 573 K. The results thus suggest that a more active bond-breaking mechanism may be operating for Ru – for example, path 1, while the less reactive path 2 may be operating for Pd. Moreover, a band at 1545 cm<sup>-1</sup> is present at 573 K and 673 K for Pd, which is consistent with the earlier proposal that a  $\nu(\text{OCO})$  mode of a carboxylate-like species forms from the

interlocking of the carbonyl of the keto tautomer intermediate (i.e., 2,4-cyclohexadienone) with defect sites of zirconia, predisposing the molecule to attack of the carbonyl functional group to hydrogenation to 2,4-cyclohexadienol. Formation of the latter facilitates formation of benzene by dehydration.

DRIFTS spectra of the Pt catalyst bear many similarities, but some differences, to Pd. The carboxylate-like band as previously described for Pd was detected at 573 K (~1537 cm<sup>-1</sup>). However, the ratio of cyclohexanol bands to phenoxy bands was higher for Pt versus Pd at least up to 473 K, and broad low-lying bands in the range of  $\nu(\text{C=O})$  (e.g., 1620 – 1800 cm<sup>-1</sup>) were detected up to 573 K in the case of Pt. These results are consistent with the higher selectivities to cyclohexanone (and its subsequent hydrogenation product, cyclohexanol) and lower selectivity to benzene for Pt relative to Pd (Table 3).

In comparison with Pd and Pt, the cyclohexanol to phenoxy band ratio is even greater for Rh up to 473 K. However, at 573 K, cyclohexanol bands are virtually absent for Rh, whereas they are clearly present for Pd and detected at low intensity with Pt. Likewise, phenoxy bands were barely discernible, as was a broad band peaking at 1614 but extending up to 1680 cm<sup>-1</sup>, which may be ascribed to  $\nu(\text{C=O})$ . The latter is consistent with the formation of cyclohexanone (Table 3). In comparison with Pt and Pd, results for Rh at 573 K suggest that it is more reactive than the other two metals. Further evidence for this conclusion is the higher methane selectivity, as well as the significantly higher C<sub>5</sub>-C<sub>6</sub> hydrocarbon selectivities (Table 3).

## FULL PAPER



## FULL PAPER

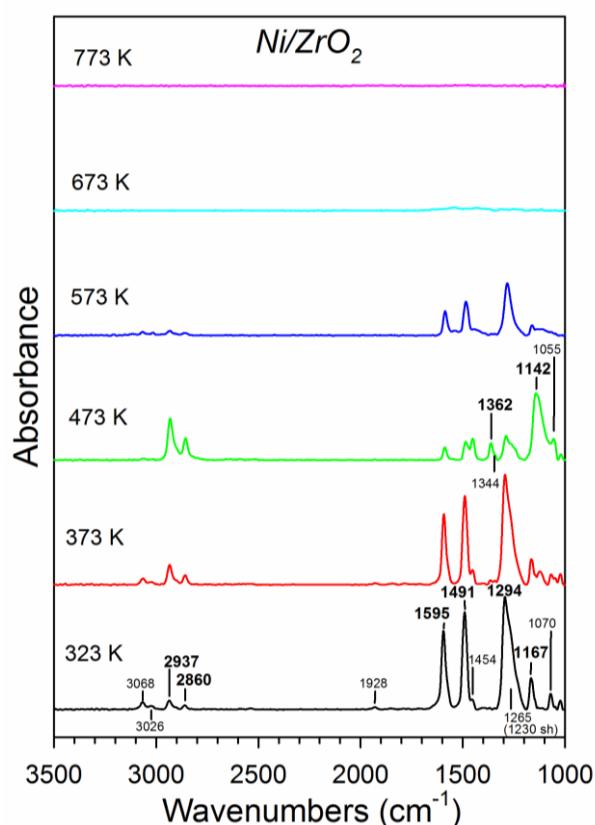


**Figure 2.** DRIFTS spectra obtained under reaction mixture containing phenol and hydrogen ( $H_2$ /phenol molar ratio = 60) at different temperatures (323, 373, 473, 573, 673 K) over Pt/ZrO<sub>2</sub>; Pd/ZrO<sub>2</sub>; Rh/ZrO<sub>2</sub>; Ru/ZrO<sub>2</sub> and Ni/ZrO<sub>2</sub> catalysts.

As in the case of Ru, the summation of band intensities for Ni reveals a lower coverage, which may indicate that Ni is carrying out more active bond breaking reactions. In agreement with this, and consistent with path 1, the selectivity to methane was quite high (albeit approximately half that of Ru), and C<sub>5</sub>-C<sub>6</sub> hydrocarbons were formed. However, judging from the infrared band intensities, there remains a low coverage of adsorbed cyclohexanol and phenoxy bands on the Ni catalyst at 573 K. These species are likely responsible for the cyclohexanone, cyclohexanol, and possibly benzene that is produced from pathway 2.

#### Proposed reaction pathway for hydrodeoxygenation of phenol

The reaction mechanism for HDO of phenol has been debated in the open literature.<sup>[2a,5,18,19]</sup> Different reaction pathways have been proposed for the HDO of phenol such as: (i) successive metal-catalyzed steps for hydrogenating (HYD) the aromatic ring and acid-catalyzed dehydration of the cyclohexanol formed. This route depends strongly on the acidity of the support. [14b,20] Zirconia does not offer a significant extent of dehydration due to insufficient acidity, as revealed by the catalytic tests with the pure support; (ii) the direct deoxygenation (DDO) that involves high

dissociation energy of the C-O bond of the aromatic ring in the phenol molecule and thus, it may occur depending on reaction temperature and catalyst used; and (iii) the phenol tautomerization to a 2,4-cyclohexadienone intermediate.<sup>[5]</sup> At this stage, 2,4-cyclohexadienone may be hydrogenated at the ring to produce 2-cyclohexen-1-one, which is further hydrogenated (e.g., to cyclohexanone and cyclohexanol), or with the right catalyst surface structure be preferentially hydrogenated at the carbonyl group. This produces 2,4-cyclohexadienol, which is subsequently dehydrated to benzene.

The results obtained in the present work revealed that the reaction pathway for HDO of phenol strongly depends on the type of metal. Similar results have been reported in the literature for HDO of different model molecules.<sup>[2e,f,i,l,17,21]</sup>

Silica supported metal catalysts (i.e., Ni, Pd, and Pt) were investigated for m-cresol HDO.<sup>[40]</sup> The main products formed at 573K were toluene and 3-methylcyclohexanone over Pt- and Pd-based catalysts. However, a high selectivity to methane and phenol was also observed for Ni/SiO<sub>2</sub> catalyst. Direct deoxygenation producing toluene and hydrogenation (forming methylcyclohexanone and/or methylcyclohexanol) were suggested by Chen et al.[19d] to be the major reactions, with selectivity depending on the metal. They suggested that deoxygenation occurs through a mechanism that may involve direct C-O hydrogenolysis or tautomerization, because there was insufficient acidity to catalyze 3-methylcyclohexanol for a hydrogenation/deoxygenation pathway. Scission of the C-C bond by hydrogenolysis of the m-cresol methyl group over Ni catalyst yielded methane and phenol. However, the reasons for the higher hydrogenolysis activity on Ni/SiO<sub>2</sub> catalyst were not given.

A detailed investigation about the HDO of m-cresol in gas phase over silica supported catalysts (Pd, Pt, Ru, Ni, Fe, NiFe) is available in the literature.<sup>[5,17,22]</sup> Products of hydrogenation (e.g., 3-methylcyclohexanone and 3-methylcyclohexanol) were mainly formed over Pt/SiO<sub>2</sub>, Pd/SiO<sub>2</sub> and Ni/SiO<sub>2</sub> catalysts whereas toluene was the main product on Fe and Ni-Fe bimetallic catalysts. Ru/SiO<sub>2</sub> catalyst also exhibited a high selectivity to toluene, CH<sub>4</sub> and C<sub>2</sub>-C<sub>6</sub> hydrocarbons. Differences in product distributions were attributed to a complex reaction pathway that varied depending on the type of metal. For Pt/SiO<sub>2</sub>, Pd/SiO<sub>2</sub>, Ni/SiO<sub>2</sub>, Fe/SiO<sub>2</sub>, NiFe/SiO<sub>2</sub> catalysts, the formation of a keto-tautomer intermediate (3-methyl-3,5-cyclohexadienone) is a key step, followed by the hydrogenation of the ring of this tautomer, producing 3-methylcyclohexanone, or the hydrogenation of the carbonyl group, originating 3-methyl-3,5-cyclohexadienol. The mechanism depends on metal type. With an oxophilic metal, such as the partially reduced Fe species in NiFe/SiO<sub>2</sub> catalysts, hydrogenation of the carbonyl group of the tautomer intermediate was favored. In contrast, the direct dehydroxylation of m-cresol occurs over Ru based catalyst. Computational studies involving DFT indicated a higher reaction energy and energy barrier for carbonyl group hydrogenation of the keto tautomer; this is due to the greater strength of the interaction between O of the carbonyl and Ru than Pt. The direct dehydroxylation was suggested to produce partially unsaturated hydrocarbon species; which may further react to toluene via hydrogenation or undergo C-C scission (yielding light hydrocarbons like methane). Thus, the oxophilicity

## FULL PAPER

of the metal surface plays a key role in determining which reaction pathway is favored. In summary, oxophilic metals such as Ru and Fe promote the deoxygenation whereas tautomerization/hydrogenation is favored over less oxophilic metals (e.g., Pt, Pd). Note that this reaction route may be further extended to explain the formation of hydrogenolysis products on some catalysts.

Concerning the HDO of phenol, there are only two studies in the literature investigating the effect of the metal on the reaction mechanism.<sup>[2e,4]</sup> Recently, we investigated the HDO of phenol reaction over a series of silica supported metal (Pd, Pt, Rh, Ru, Ni, Co) catalysts.<sup>[4]</sup> The formation of hydrogenated products (cyclohexanone and cyclohexanol) was favored over Pt/SiO<sub>2</sub>, Pd/SiO<sub>2</sub> and Rh/SiO<sub>2</sub> catalysts, whereas significant formation of hydrogenolysis products (C<sub>5</sub>-C<sub>6</sub> hydrocarbons and methane) was observed over Co/SiO<sub>2</sub>, Ni/SiO<sub>2</sub> and mainly Ru/SiO<sub>2</sub> catalysts. These results showed that the reaction pathway depends on the type of the metal. With silica supported Pt, Pd, and Rh, phenol undergoes tautomerization, with subsequent hydrogenation of the ring. The direct dehydroxylation of phenol followed by hydrogenolysis is favored over more oxophilic metals (Ru, Co and Ni). To establish a relation between HDO activity and oxophilicity of the metals in terms of the ability to bind with O from the carbonyl functional group, the selectivity to deoxygenated products was investigated as a function of the binding energy of atomic oxygen calculated by Lee et al.<sup>[23]</sup> The following order for selectivity to deoxygenated products was observed (in parentheses are reported the binding energies of atomic oxygen): Ru (-5.90) > Co (-5.58) > Ni (-5.40) > Rh (-5.04) > Pd (-4.48) > Pt (-4.20). This result reveals that the more oxophilic the metal, the higher the selectivity to deoxygenated products. As observed by Tan et al.<sup>[17]</sup> and Hensley et al.<sup>[24]</sup>, the stronger interaction between the oxygen from carbonyl group to metal favors the formation of deoxygenated products.

In the present work, both reaction pathways (tautomerization and direct deoxygenation) might take place and the importance of each one will depend on the type of the metal. For Pd/ZrO<sub>2</sub> and Pt/ZrO<sub>2</sub> catalysts, tautomerization is the reaction pathway favored, as recently demonstrated by the formation of tautomer intermediate during the HDO of phenol reaction.<sup>[5]</sup> The high formation of methane and C<sub>5</sub>-C<sub>6</sub> hydrocarbons over Ru/ZrO<sub>2</sub>, Ni/ZrO<sub>2</sub> and Co/ZrO<sub>2</sub> catalysts could be attributed to the direct dehydroxylation of phenol followed by hydrogenolysis of the intermediate formed. According to the mechanism proposed by Tan et al.<sup>[17]</sup>, the direct deoxygenation of m-cresol produces an unsaturated hydrocarbon surface species that undergoes hydrogenolysis to C<sub>1</sub>-C<sub>5</sub> hydrocarbons; or it can be hydrogenated, forming toluene. The hydrogenolysis reaction proceeds by cleaving C-C bonds to form C<sub>x</sub>H<sub>y</sub> species and CH species. The hydrogenolysis of alkanes has been considered a structure-sensitive reaction and a decrease in activity with decreasing particle size has been observed.<sup>[25]</sup> Iglesia's group performed a detailed study about the hydrogenolysis of n-alkanes on Ir, Rh and Pt clusters.<sup>[25a,26]</sup> They used statistical mechanics and transition state theory to determine the rates and selectivities of C-C bond cleavage in C<sub>2</sub>-C<sub>10</sub> n-alkanes to describe the hydrogenolysis of hydrocarbons. They reported that large metal clusters exhibit

higher hydrogenolysis rates due to the weaker bonding of H<sup>+</sup> atoms to terrace sites.

In order to demonstrate that direct deoxygenation takes place over Ru-based catalysts, a 1%Ru/ZrO<sub>2</sub> catalyst with smaller Ru particle size was tested for HDO of phenol and the results are presented in Table 3. The decrease in Ru particle size was accompanied by a significant reduction in the formation of methane and C<sub>5</sub>-C<sub>6</sub> hydrocarbons as well as by an increase in the selectivity to benzene. This result agrees very well with the work of Newman et al.<sup>[29]</sup> They reported that a Ru/TiO<sub>2</sub> catalyst with higher dispersion exhibited high selectivity toward direct deoxygenation. Therefore, the selectivity to methane and C<sub>5</sub>-C<sub>6</sub> hydrocarbons could be used to measure the extent of the direct deoxygenation reaction pathway for HDO of phenol reaction. For the catalysts that do not exhibit significant hydrogenolysis reaction (Pt/ZrO<sub>2</sub>, Pd/ZrO<sub>2</sub>, Rh/ZrO<sub>2</sub>), the changes in product distribution are not due to the different metal dispersion. For these catalysts, the hydrogenation was the main reaction, which is considered an insensitive structure-reaction. Recently, the effect of Pd particle size on the product distribution for HDO of phenol in gas phase over Pd/ZrO<sub>2</sub> catalysts with different Pd dispersions was investigated.<sup>[5]</sup> Similar selectivities were observed with both catalysts; thus, the dispersion of the metal does not significantly affect the HDO product distribution. But the effect of the metal dispersion on HDO of phenol reaction is controversial in the literature. In addition, When Co/ZrO<sub>2</sub> is compared with the Ni/ZrO<sub>2</sub> catalyst with approximately the same dispersion, it is clear that the differences in product distribution are due to the type of the metal.

However, the order observed for the selectivity to deoxygenated products for zirconia supported catalysts was not the same as that obtained for the silica supported catalysts from our previous study<sup>[4]</sup> (Fig. 3). For silica supported catalysts, Ni exhibits a higher selectivity to deoxygenated products than Rh, which is reasonable since Ni is more oxophilic than Rh. However, this is not observed for Ni/ZrO<sub>2</sub> and Rh/ZrO<sub>2</sub> catalysts. Even Pt and Pd metals, which did not produce benzene when supported on silica, showed significant formation of deoxygenated products in the presence of zirconia. This result reveals the important role the support for the HDO of phenol reaction. Griffin et al.<sup>[27]</sup> also observed a high selectivity to toluene for HDO of m-cresol when Pt was supported on TiO<sub>2</sub>. They proposed that tautomerization and direct deoxygenation to toluene were energetically favorable routes over TiO<sub>2</sub> (101) surfaces. In this case, the reaction takes place at oxygen vacancy defects. For the Pt(111) surface, 3-methylcyclohexanone and 3-methylcyclohexanol were mainly formed by the hydrogenation of the ring, which explains the low selectivity to toluene for the Pt/C catalyst used.

In the present work, in addition to the metal, the support also provides oxophilic sites that will take part in the reaction mechanism. This explains the higher formation of deoxygenated products for the HDO of phenol over zirconia supported catalysts. There are some studies in the literature that report the promoting effect of oxophilic sites for the deoxygenation activity. For instance, the high selectivity to benzene for the HDO of phenol in the liquid phase over Ru/TiO<sub>2</sub> catalyst was attributed to the strong interaction between the Ti<sup>3+</sup> sites (created during the reduction)

## FULL PAPER

with the oxygen from the phenol molecule that weakened the C-O bond.

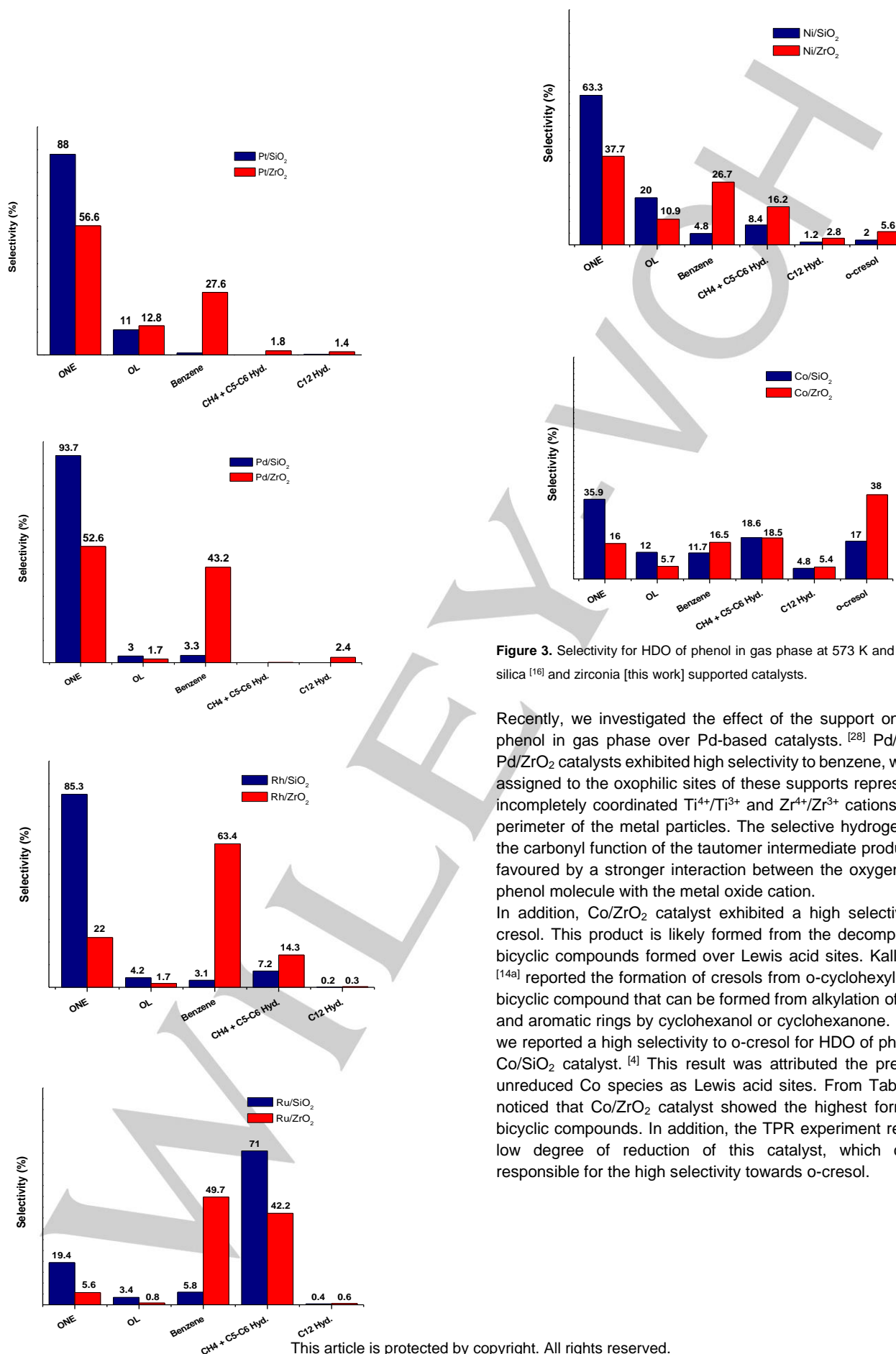


**Figure 3.** Selectivity for HDO of phenol in gas phase at 573 K and 1 atm over silica [16] and zirconia [this work] supported catalysts.

Recently, we investigated the effect of the support on HDO of phenol in gas phase over Pd-based catalysts. [28] Pd/TiO<sub>2</sub> and Pd/ZrO<sub>2</sub> catalysts exhibited high selectivity to benzene, which was assigned to the oxophilic sites of these supports represented by incompletely coordinated Ti<sup>4+</sup>/Ti<sup>3+</sup> and Zr<sup>4+</sup>/Zr<sup>3+</sup> cations near the perimeter of the metal particles. The selective hydrogenation of the carbonyl function of the tautomer intermediate produced was favoured by a stronger interaction between the oxygen atom in phenol molecule with the metal oxide cation.

In addition, Co/ZrO<sub>2</sub> catalyst exhibited a high selectivity to o-cresol. This product is likely formed from the decomposition of bicyclic compounds formed over Lewis acid sites. Kallury et al. [14a] reported the formation of cresols from o-cyclohexylphenol, a bicyclic compound that can be formed from alkylation of phenolic and aromatic rings by cyclohexanol or cyclohexanone. Recently, we reported a high selectivity to o-cresol for HDO of phenol over Co/SiO<sub>2</sub> catalyst. [4] This result was attributed the presence of unreduced Co species as Lewis acid sites. From Table 3, it is noticed that Co/ZrO<sub>2</sub> catalyst showed the highest formation of bicyclic compounds. In addition, the TPR experiment revealed a low degree of reduction of this catalyst, which could be responsible for the high selectivity towards o-cresol.

## FULL PAPER

**Stability of supported metallic catalysts on HDO of phenol**

The conversion of phenol and product distribution as a function of time on stream (TOS) for all catalysts are shown in Fig. 4. All catalysts deactivated during 24 h of TOS but the main deactivation occurs at the beginning of reaction (before 200 min.). In addition, the deactivation degree depended on the metal. The stability of the catalysts defined by Eq. (3) was calculated and the following order was obtained: Pd/ZrO<sub>2</sub> (0.58) > Pt/ZrO<sub>2</sub> (0.41) > Co/ZrO<sub>2</sub> (0.39) > Rh/ZrO<sub>2</sub> (0.35) > Ru/ZrO<sub>2</sub> (0.24) > Ni/ZrO<sub>2</sub> (0.19). Furthermore, the selectivities significantly changed with TOS. The selectivity to cyclohexanone increased and the formation of benzene decreased as the phenol conversion decreased for Pt, Pd, Rh, Ni catalysts. The selectivity to C<sub>12</sub> hydrocarbons also decreased with TOS. For Ru/ZrO<sub>2</sub>, the selectivity to CH<sub>4</sub> strongly decreased at the beginning of reaction, whereas it slightly diminished for the other catalysts.

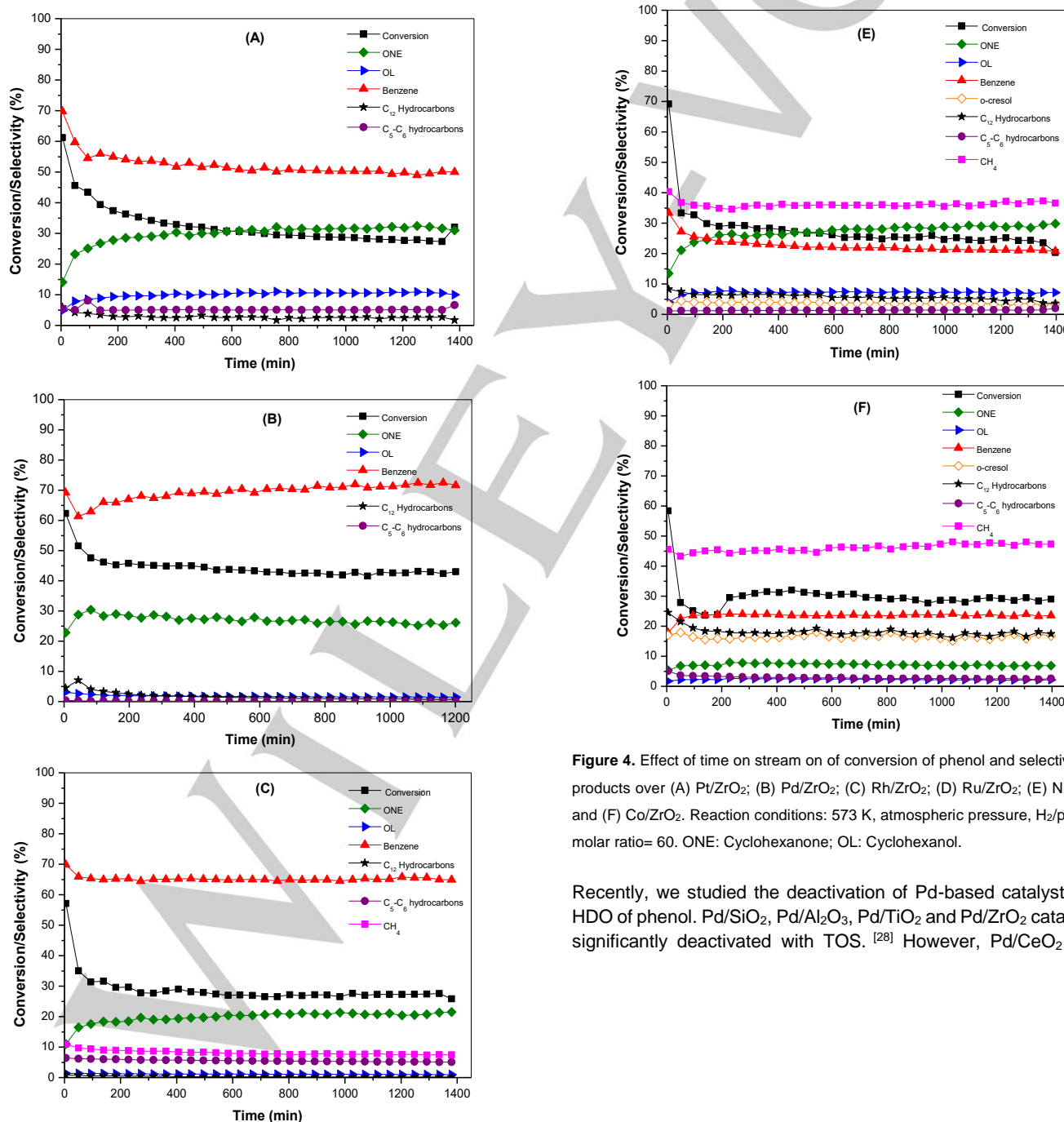


**Figure 4.** Effect of time on stream on of conversion of phenol and selectivity of products over (A) Pt/ZrO<sub>2</sub>; (B) Pd/ZrO<sub>2</sub>; (C) Rh/ZrO<sub>2</sub>; (D) Ru/ZrO<sub>2</sub>; (E) Ni/ZrO<sub>2</sub> and (F) Co/ZrO<sub>2</sub>. Reaction conditions: 573 K, atmospheric pressure, H<sub>2</sub>/phenol molar ratio= 60. ONE: Cyclohexanone; OL: Cyclohexanol.

Recently, we studied the deactivation of Pd-based catalysts for HDO of phenol. Pd/SiO<sub>2</sub>, Pd/Al<sub>2</sub>O<sub>3</sub>, Pd/TiO<sub>2</sub> and Pd/ZrO<sub>2</sub> catalysts significantly deactivated with TOS. [28] However, Pd/CeO<sub>2</sub> and

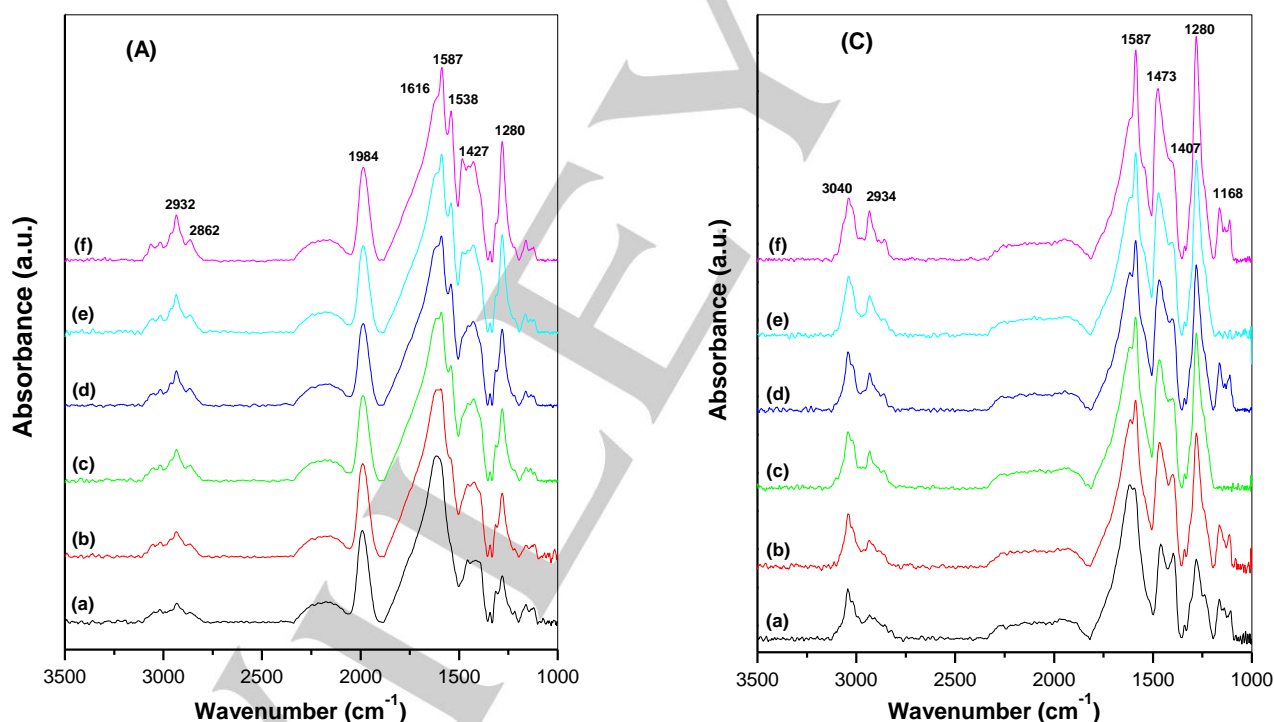
## FULL PAPER

Pd/CeZrO<sub>2</sub> were more stable and only slight losses in activity were observed. Carbon deposits were not detected by Raman spectroscopy after reaction. DRIFTS experiments under reaction conditions revealed a build-up of phenoxy and intermediate species during reaction. These species remained adsorbed on the oxophilic sites, blocking those sites and inhibiting further reactant adsorption.

The growth of Pd particle size and a decrease in the density of oxophilic sites during the HDO of phenol were the main causes of catalyst deactivation.

Therefore, in the present study, DRIFTS experiments under reaction conditions were carried out in order to monitor the evolution of adsorbed species.

Fig. 5 show the DRIFTS spectra for HDO of phenol at 573 K. Bands of adsorbed phenoxy species were detected for all catalysts. In all cases, except that of Ru, bands of adsorbed cyclohexanol were also evidenced. In addition, the  $\nu(\text{C}=\text{O})$  band of cyclohexanone was observed for the Pt and Rh catalysts as a high wavenumber shoulder; furthermore, the Pt-carbonyl band was identified at 1984 cm<sup>-1</sup>. These key bands tended to increase with TOS. The build-up of an inventory of intermediates on the catalyst surface suggests that the turnover rate of these species is slowly becoming hindered with TOS. The sharpest increases in inventory followed the trend: Ru > Ni > Rh > Pt > Pd. These results are consistent with the initial deactivation trends observed in the long-term catalytic tests, with Ru offering the steepest initial decline, and Pd offering the greatest stability.



## FULL PAPER

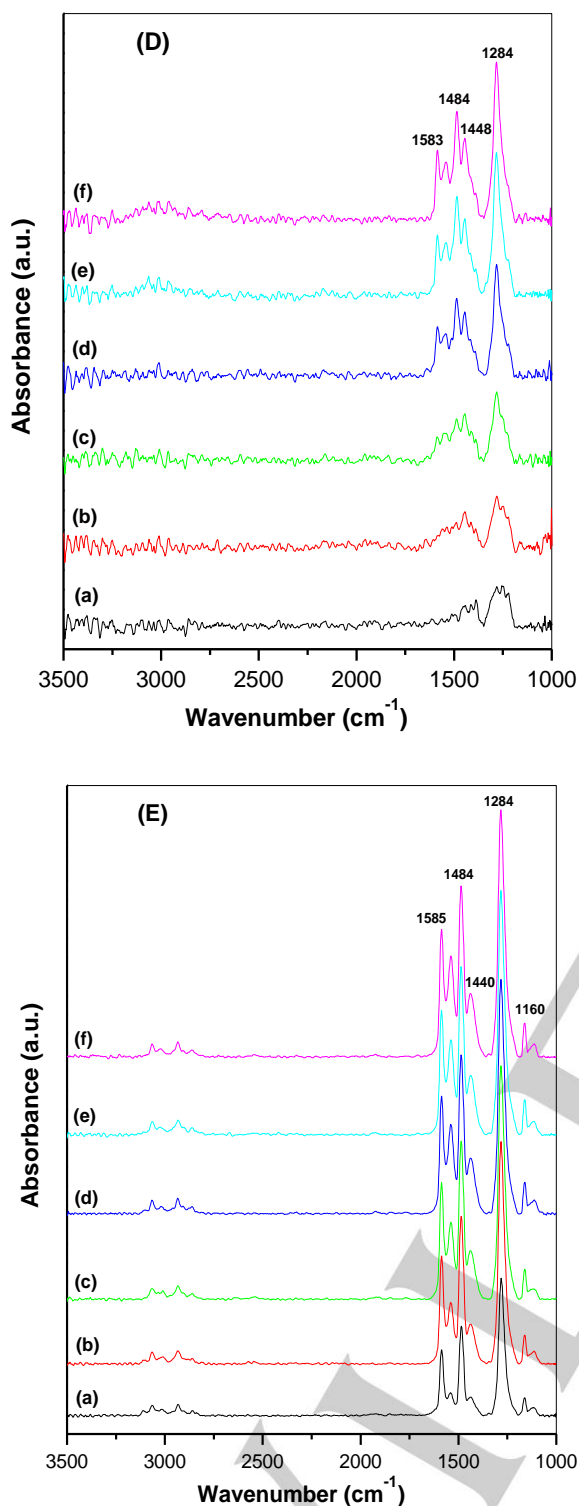


**Figure 5.** DRIFTS spectra obtained at 573 K and under the reaction mixture containing phenol and hydrogen during 6 h TOS: (a) 60; (b) 120; (c) 180; (d)

240; (e) 300; (f) 360 over (A) Pt/ZrO<sub>2</sub>; (B) Pd/ZrO<sub>2</sub>; (C) Rh/ZrO<sub>2</sub>; (D) Ru/ZrO<sub>2</sub>; (E) Ni/ZrO<sub>2</sub>.

Therefore, DRIFTS experiments revealed the build-up of intermediate species on the surface of all catalysts. This could be caused by the loss of the Pd-support interaction, which could be associated with: (i) carbon deposition resulting in site blocking at the interface; (ii) metal sintering, which decreases the interface between metal particles and support; or (iii) changes in the acid sites of the support (e.g., decreases in Lewis acid sites due to site blocking by strong adsorbates).

In the present work, Raman spectra of the used catalysts did not detect the formation of carbon deposits on the surface of all catalysts.

In order to investigate the changes in metal particle size during the reaction, the dehydrogenation of cyclohexane reaction was carried out before and after the HDO of phenol reaction. The ratio between the reaction rates of dehydrogenation of cyclohexane at 543 K over fresh and used (after 24 h of TOS for HDO of phenol reaction) catalysts is reported in Table 5. The results showed a significant reduction in reaction rate, which suggest that metal particles growth contributed to catalyst deactivation. However, the degree of sintering varied depending on the metal. This was more important for Pt, Pd and Co supported catalysts. The lowest decrease in the reaction rate of dehydrogenation of cyclohexane was observed for the Ru/ZrO<sub>2</sub> and Rh/ZrO<sub>2</sub> catalysts.

**Table 5.** Ratio between the reaction rate of dehydrogenation of cyclohexane at 543 K over fresh and used catalysts and the reaction rate of dehydration of cyclohexanol at 543 K over fresh and used catalysts (after 23 h of HDO of phenol reaction).

Catalyst	Dehydrogenation of cyclohexane ratio <sup>[a]</sup>	Dehydration of cyclohexanol ratio <sup>[b]</sup>
Pt/ZrO <sub>2</sub>	18.5	6.2
Pd/ZrO <sub>2</sub>	10.1	2.5
Rh/ZrO <sub>2</sub>	2.9	8.8
Ru/ZrO <sub>2</sub>	1.4	0.9
Ni/ZrO <sub>2</sub>	5.5	7.7
Co/ZrO <sub>2</sub>	24.0	0.9

<sup>[a]</sup> Ratio between the reaction rate of dehydrogenation of cyclohexane at 543 K over fresh and used (after 23 h of HDO of phenol reaction) catalysts.

<sup>[b]</sup> Ratio between the reaction rate of dehydration of cyclohexanol at 543 K over fresh and used (after 23 h of HDO of phenol reaction) catalysts.

The changes in the density of oxophilic sites were measured by the dehydration of cyclohexanol reaction. Table 5 lists the ratio between the reaction rates for dehydration of cyclohexanol before and after HDO reaction. A significant decrease in the rate of cyclohexanol dehydration is observed for Pt/ZrO<sub>2</sub>, Rh/ZrO<sub>2</sub>, and Ni/ZrO<sub>2</sub> catalysts. For Ru/ZrO<sub>2</sub>, and Co/ZrO<sub>2</sub> catalysts, the reaction rate only slightly decreased after 20 h of TOS. The comparison between the variation of metal dispersion and the density of acid sites during HDO of phenol over all catalysts suggest that metal sintering is the main cause of catalyst deactivation. The growth of metal particle size decreases the

## FULL PAPER

metal particle-support interface that affects the ability of the adsorbed species to turnover, leading to an accumulation of phenoxy species during reaction, as revealed by DRIFTS experiments. However, the decrease in the density of acid sites is significant for Pt, Rh and Ni-based catalysts. Considering that the HDO of phenol is a bifunctional mechanism, the decrease of both the metal particle-support interface (Pd sintering) as well as the number of Lewis acid sites (site blocking) might contribute to the deactivation observed for zirconia supported catalysts during the HDO of phenol reaction.

## Conclusions

This work investigated the effect of metal type (Pt, Pd, Rh, Ru, Cu, Ni, Co) for the HDO of phenol in gas phase over zirconia supported catalysts. Activity and product distribution were significantly affected by the type of metal. While zirconia supported Pt and Pd tended to produce hydrogenated products, such as cyclohexanone and cyclohexanol, zirconia supported Rh, Co, Ni, and Ru catalysts produced significant fractions of C<sub>5</sub>, C<sub>6</sub>, and methane, as the products of hydrogenolysis. Cu/ZrO<sub>2</sub> catalyst was inactive under the reaction conditions used. Two reaction pathways (tautomerization and direct deoxygenation) might take place, the importance of each one will depend on the type of the metal. Phenol tautomerization is the main reaction pathway for Pd/ZrO<sub>2</sub> and Pt/ZrO<sub>2</sub> catalysts. The high formation of methane and C<sub>5</sub>-C<sub>6</sub> hydrocarbons over Ru/ZrO<sub>2</sub>, Ni/ZrO<sub>2</sub> and Co/ZrO<sub>2</sub> catalysts could be attributed to the direct dehydroxylation of phenol that produces an unsaturated hydrocarbon surface species. This intermediate underwent hydrogenolysis to C<sub>1</sub>-C<sub>5</sub> hydrocarbons or it can be hydrogenated, forming benzene. The selectivity to methane and C<sub>5</sub>-C<sub>6</sub> hydrocarbons could be used to measure the extent of direct deoxygenation reaction pathway for HDO of phenol.

In addition to the metals, the oxophilic sites of this support represented by incompletely coordinated Zr<sup>4+</sup> and Zr<sup>3+</sup> cations near the perimeter of the metal particles also played an important role on the selectivity to deoxygenated products. This explains the higher formation of deoxygenated products for the HDO of phenol over zirconia supported catalysts in comparison to silica supported ones.

All catalysts significantly deactivated during TOS, regardless the type of the metal. Carbon deposits were not detected by Raman spectroscopy after reaction. DRIFTS experiments under reaction conditions revealed a build-up of phenoxy and intermediate species during reaction. These species remained adsorbed on the oxophilic sites, blocking those sites and inhibiting further reactant adsorption. The growth of metal particle size decreases the metal particle-support interface that affects the ability of the adsorbed species to turnover, leading to an accumulation of phenoxy species during reaction, as revealed by DRIFTS experiments. The growth of metal particle size and a decrease in the density of oxophilic sites (site blocking by strong

adsorption of intermediates) during the HDO of phenol reaction were the main causes of catalyst deactivation.

## Experimental Section

### Catalyst synthesis

ZrO<sub>2</sub> support was synthesized by the precipitation method. A solution of 2.0 mol L<sup>-1</sup> zirconyl nitrate (35 wt.% ZrO(NO<sub>3</sub>)<sub>2</sub> in dilute nitric acid, > 99%, Sigma-Aldrich) was added slowly to a solution of 4.0 mol L<sup>-1</sup> ammonium hydroxide (NH<sub>4</sub>OH, Vetec) at room temperature, and kept under vigorous stirring for 30 min. The resulting precipitate was filtered and washed with distilled water until a pH of 7 was reached. Then, the solid was dried at 383 K for 12 h and calcined under a dry air flow at 773 K (heating ramp 5 K min<sup>-1</sup>) for 6 h.

ZrO<sub>2</sub> supported metal catalysts with a nominal Pt, Pd and Rh loading of 1.0 wt. %, Ru and Cu of 5.0 wt. %, Ni and Co of 10.0 wt. % were prepared by incipient wetness impregnation of the supports with aqueous solution of respective precursor salts (Pt(NH<sub>3</sub>)<sub>4</sub>(NO<sub>3</sub>)<sub>2</sub> (Aldrich), Pd(NO<sub>3</sub>)<sub>2</sub>·2H<sub>2</sub>O (Umicore), RhCl<sub>3</sub>·H<sub>2</sub>O (Aldrich), Ru(NO)(NO<sub>3</sub>)<sub>3</sub> (Alfa Aesar), Ni(NO<sub>3</sub>)<sub>2</sub>·6H<sub>2</sub>O (Acros), Co(NO<sub>3</sub>)<sub>2</sub>·6H<sub>2</sub>O (Acros) and Cu(NO<sub>3</sub>)<sub>2</sub>·3H<sub>2</sub>O (Aldrich)). After impregnation, the powder was dried in air at 293 K for 12 h and then calcined in air at 673 K for 3 h (2 K min<sup>-1</sup>).

### Catalyst characterization

The chemical composition of each sample was determined using a Wavelength Dispersive X-Ray Fluorescence Spectrometer (WD-XRF) S8 Tiger (Bruker) with a rhodium tube operated at 4 kW. The analyses were performed with the samples (300 mg) in powder form using a semi-quantitative method (QUANT-EXPRES/Bruker). Specific surface areas of the samples were measured on a Micromeritics ASAP 2020 analyzer by N<sub>2</sub> adsorption at the boiling temperature of liquid nitrogen. The X-ray powder diffraction (XRD) patterns were obtained using a Rigaku diffractometer with Cu K $\alpha$  radiation ( $\lambda$  = 1.5406 Å) over a 2 $\theta$  range of 10-80° at a scan rate of 0.04 °/step and a scan time of 1 s/step. TPR experiments were performed in a TPR/TPD 2900 Micromeritics system equipped with a thermal conductivity detector (TCD). The catalyst was pretreated at 673 K for 1 h under a flow of air prior to the TPR experiment to remove adsorbed species from the catalyst surface. The reducing mixture (10.0 % H<sub>2</sub>/N<sub>2</sub>) was passed through the sample (100 mg) at a flow rate of 30 mL min<sup>-1</sup> and the temperature was increased to 1273 K at a heating rate of 10 K min<sup>-1</sup>. The metal dispersion was measured by H<sub>2</sub> chemisorption at 298 K for Rh, Pt, Ru, Ni, Co-based catalysts using a Micromeritics apparatus. Before adsorption, the samples were reduced under pure H<sub>2</sub> (60 ml min<sup>-1</sup>) at 773 K for 1h (10 K.min<sup>-1</sup>), followed by evacuation for 30 min and cooling to room temperature. Irreversible uptakes at 298 K were determined from the dual isotherms measured for hydrogen. First, the total adsorption was determined at 298 K and the catalyst was outgassed for 30 min, after which a new isotherm was measured. Then, the difference between both isotherms was extrapolated to zero pressure to calculate the amount of hydrogen adsorbed, considering a stoichiometry H/Me = 1. This method was not used for the determination of Pd dispersion due to the formation of hydride in palladium. In this case, the dehydrogenation of cyclohexane was used as an insensitive structure reaction to determine the metal dispersion of supported Pd catalysts.<sup>[5,12]</sup> This procedure enables the measurement of

## FULL PAPER

the metal dispersion of fresh and used catalysts (after HDO of phenol for 24 h). This reaction was performed in a fixed bed reactor at atmospheric pressure. The fresh samples were first reduced at 773 K for 1 h and then cooled to the cyclohexane dehydrogenation reaction temperature (543 K). The reaction mixture was fed to the reactor after bubbling H<sub>2</sub> through a saturator containing cyclohexane kept at 285 K (H<sub>2</sub>/C<sub>6</sub>H<sub>12</sub> = 13.2). For the used catalysts, after HDO of phenol for 24 h, the saturator containing phenol was bypassed and hydrogen flowed through the catalyst for 30 min at 573 K, which removed hydrocarbons that remained adsorbed on the surface. The reactor was cooled to 543 K under hydrogen. Then, a cyclohexane/H<sub>2</sub> mixture was passed through the reactor. The exit gases were analyzed by an Agilent Technologies 7890A/5975C CGMS, using a HP-Innowax capillary column and a flame-ionization detector (FID).

The titration of oxophilic sites of the catalysts before and after HDO of phenol was measured by conducting the cyclohexanol dehydration reaction.<sup>[13]</sup> The reaction was performed using a fixed-bed quartz reactor at atmospheric pressure and 543 K. Prior to reaction, the fresh catalyst was reduced *in situ* under pure hydrogen (60 mL min<sup>-1</sup>) at 573 K for 1 h. The used catalysts were not exposed to air before starting the cyclohexanol reaction. The reactant mixture was obtained by flowing He (30 mL min<sup>-1</sup>) through a saturator containing cyclohexanol, which was maintained at 336 K. The reaction products were analyzed by GCMS (Agilent Technologies 7890A/5975C) using an HP-Innowax capillary column and a flame-ionization detector (FID). The dehydration rate was calculated by the sum of cyclohexene, cyclohexane and benzene yields.

To investigate the reaction mechanism, experiments were performed in an *in situ* DRIFTS cell (Thermo Spectra-Tech high P/high T with ZnSe windows) using a Nicolet Nexus 870 spectrometer equipped with a DTGS-TEC detector under similar conditions to those employed in the HDO reaction. Scans were taken at a resolution of 4 cm<sup>-1</sup> to give a data spacing of 1.928 cm<sup>-1</sup>. The number of scans taken was 1024. The amount of catalyst was ~ 40 mg. The sample was reduced in H<sub>2</sub> at 773 K for 1 h and cooled to 323 K in He, and a background spectrum was recorded. Pure H<sub>2</sub> was then flowed through a bubbler containing phenol at 351 K and the temperature was raised to 373, 473, 573, 673 and 773 K. To study the deactivation of the catalysts, several spectra were recorded during the steady-state HDO reaction at 573K for 6 h using a H<sub>2</sub> flow of 60 ml min<sup>-1</sup> through the phenol saturator.

### Catalytic activity

The vapor-phase conversion of the oxygenate compound of interest (phenol, cyclohexanol, or cyclohexanone) was carried out in a fixed-bed quartz reactor, operating at atmospheric pressure and 573 K. Prior to reaction, the catalyst was reduced *in situ* under pure hydrogen (60 mL min<sup>-1</sup>) at 773 K for 1 h. The catalysts were diluted with inert material (SiC mass/catalyst mass = 3.0) to avoid hot-spot formation. The reactant mixture was obtained by flowing H<sub>2</sub> through the saturator containing organic compound, which was kept at the specific temperature required to obtain the desired H<sub>2</sub>/organic compound molar ratio (about 60). To avoid condensation, all lines were heated at (523 K). The reaction products were analyzed by GC-MS (Agilent Technologies 7890A), using an HP-Innowax capillary column and a flame-ionization detector (FID). Each of the catalysts investigated was evaluated at different W/F by varying the catalyst amount in the range of 2.5-120 mg. The W/F is defined as the ratio of the catalyst mass (g) to the mass flow rate of the organic feed (g/h). The product yield and selectivity for each product were calculated as follows:

$$\text{yield}(\%) = \frac{\text{mol of product produced}}{\text{mol of phenol fed}} \times 100 \quad (1)$$

$$\text{Selectivity}(\%) = \frac{\text{mol of product produced}}{\text{mol of phenol consumed}} \times 100 \quad (2)$$

$$\text{Stability} = \ln(1 - X_{(t)}) / \ln(1 - X_{(t_0)}) \quad (3)$$

### Acknowledgements

The authors thank CAPES (Coordenação de Aperfeiçoamento de Pessoal de Ensino Superior) and CNPq (Conselho Nacional de Desenvolvimento Científico e Tecnológico) for supporting this research and the scholarship received. CAER researchers would like to thank the Commonwealth of Kentucky for support.

**Keywords:** Dehydroxylation • Hydrodeoxygenation • Phenol • Tautomerization • ZrO<sub>2</sub>

- [1] X. Zhu, L. Nie, L. L. Lobban, R. G. Mallinson, D. E. Resasco, *Energy Fuels* **2014**, *28*, 4104-4111.
- [2] a) J. He, C. Zhao, J. A. Lercher, *J. Catal.* **2014**, *309*, 362-375; b) C. R. Lee, J. S. Yoon, Y. W. Suh, J. W. Choi, J. M. Ha, D. J. Suh, Y. K. Park, *Catal. Comm.* **2012**, *17*, 54-58; c) D. H. Hong, S. J. Miller, P. K. Agrawal, C. W. Jones, *Chem. Comm.* **2010**, *46*, 1038-1040; d) J. Horacek, G. St'ávoová, V. Kelbichová, D. Kubicka, *Catal. Today* **2013**, *204*, 38-45; e) P. M. Mortensen, J.-D. Grunwaldt, P. A. Jensen, A. D. Jensen, *ACS Catal.* **2013**, *3*, 1774-1785; f) T. Mochizuki, S. Chen, M. Toba, Y. Yoshimura, *Appl. Catal. B: Environ.* **2014**, *146*, 237-243; g) C. Newman, X. Zhou, B. Goundie, I. T. Ghampson, R. A. Pollock, Z. Ross, M. C. Wheeler, R. Meulenberg, R. N. Austin, B. G. Frederick, *App. Catal. A: Gen.* **2014**, *477* 64-74; h) J. Filley, C. Roth, *J. Mol. Catal. A: Chem.* **1999**, *139*, 245-252; i) C. Zhao, J. He, A. A. Lemonidou, X. Li, J. Lercher, *J. Catal.* **2011**, *280*, 8-16; j) J. Sun, A. M. Karim, H. Zhang, L. Kovarik, X. S. Li, A. J. Hensley, J. S. Mcewen, J. Wang, *J. Catal.* **2013**, *47-57*; k) X. Zhang, T. Wang, L. Ma, Q. Zhang, Y. Yu, Q. Liu, *Catal. Comm.* **2013**, *33*, 15-19; l) B. Guvenatam, O. Kursun, E. H. J. Heeres, E. A. Pidko, E. J. M. Hensen, *Catal. Today* **2013**, *233*, 83-91; m) S. Echeandia, B. Pawelec, V. L. Barrio P. L. Arias, J. F. Cambra, C. V. Loricera, J. L. G. Fierro, *Fuel* **2014**, *117*, 1061-1073.
- [3] J. K. Nørskov, J. Rossmeisl, A. Logadottir, L. Lindqvist, *J Phys Chem B* **2007**, *108*: 17886-17892.
- [4] C. A. Teles, R. C. R. Neto, J. R. Lima, L. V. Mattos, D. E. Resasco, F. B. Noronha, *Catal. Lett.* **2016**, doi:10.1007/s10562-016-1815-5.
- [5] P. M. De Souza, R. C. Rabelo-Neto, L. E. P. Borges, G. Jacobs, B. H. Davis, T. Sooknoi, D. E. Resasco, F. B. Noronha, *ACS Catal.* **2015**, *5*, 1318-1329.
- [6] W. Khaodee, B. Jongsomjit, P. Praserttham, S. Goto, S. Assabumrungrat, *J. Mol. Catal. A: Chem.* **2008**, *280*, 35-42.
- [7] a) L. V. Mattos, E. R. De Oliveira, P. D. Resende, F. B. Noronha, *Catal. Today* **2002**, *77*, 246-246; b) S. Sitthisa, D. E. Resasco, *Catal. Lett.* **2011**, *141*, 784-791; c) X. Karatzas, K. Jansson, A. Gonzalez, J. Dawody, L. Pettersson, *J. App. Catal. B: Environ.* **2011**, *106*, 476-487.
- [8] a) L. Chen, H. Zhu, H. Zheng, C. Zhang, Y. Li, *App. Catal. A: Gen* **2012**, *411-412*, 95-104; b) Y. H. Kim, E. D. Park, H. C. Lee, D. Lee, *App. Catal. A: Gen.* **2009**, *366*, 363-369.

## FULL PAPER

- [9] X. Zhang, T. Wang, L. Ma, Q. Zhang, Y. Yu, Q. Liu, *Catal. Comm.* **2013**, 33, 15-19.
- [10] T. L. Lai, Y. Y. Shu, G. L. Huang, C. C. Lee, C. B. Wang, *J. All. Comp.* **2008**, 450 (1-2), 318-322.
- [11] H. Song, L. Zhang, U. S. Ozkan, *Green Chem.* **2007**, 9, 686-694.
- [12] P. M. De Souza, R. C. R. Neto, L. E. P. Borges, G. Jacobs, B. H. Davis, U. M. Graham, D. E. Resasco, F. B. Noronha, *ACS Catal.* **2015**, 5, 7385-7398.
- [13] D. Martin, D. Duprez, *J. Mol. Catal. A: Chem.* **1997**, 118, 113-128.
- [14] a) R. K. M. R. Kallury, T. T. Tidwell, *Can. J. Chem.* **1984**, 62, 2540-2545; b) C. Zhao, D. M. Camaioni, J. A. Lercher, *J. Catal.* **2012**, 288, 92.
- [15] T. Nimmanwudipong, R. C. Runnebaum, K. Tay, D. E. Block, B. C. Gates, *Catal. Lett.* **2011**, 141, 1072-1078.
- [16] a) B-Q. Xu, T. Yamaguchi, K. Tanabe, *Mater. Chem. Phys.* **1988**, 19, 291-297; b) A. Popov, E. Kondratieva, J. M. Goupil, L. Mariey, P. Bazin, J-P. Gilson, A. Traver, F. Maugé, *Journal Phys. Chem. C* **2016**, 114, 15661-15670; c) W. Roth, P. Imhof, M. Gerhards, S. Schumm, K. Kleiner, *Chem. Phys.* **2000**, 252, 247-256.
- [17] Q. Tan, G. Wang, L. Nie, A. Dinse, C. Buda, J. Shabaker, D. E. Resasco, *ACS Catal.* **2015**, 5, 11, 6271-6283.
- [18] F. E. Massoth, P. Politzer, M. C. Concha, J. S. Murray, J. Jakowski, J. Simons, *J. Phys. Chem. B* **2006**, 110, 14283-14291.
- [19] a) C. Zhao, Y. Kou, A. A. Lemonidou, X. Li, J. Lercher, *Ang. Chem.* **2009**, 121, 4047-4050; b) X. Zhang, T. Wang, L. Ma, Q. Zhang, X. Huang, Y. Yu, *App. Energy* **2013**, 112, 533; c) J. Matos, A. Corma, *App. Catal. A: Gen.* **2011**, 404, 103-112; d) C. Chen, G. Chen, F. Yang, H. Wang, J. Han, Q. Ge, X. Zhu, *Chem. Eng. Sci.* **2015**, 135, 145-154; e) K. L. Deutsch, B. H. Shanks, *App. Catal. A: Gen.* **2012**, 447, 144-150.
- [20] A. F. Foster, P. T. M. Do, R. F. Lobo, *Top. Catal.* **2012**, 55, 118-128.
- [21] a) D. Gao, C. Schweitzer, H. T. Wang, H. A. Varma, *Ind. Eng. Chem. Res.* **2014**, 53, 18658-18667; b) Y. K. Hong, D. W. Lee, H. J. Eom, Y. K. Lee, *App. Catal. B: Environ.* **2014**, 150-151, 438-445.
- [22] L. Nie, P. M. De Souza, F. B. Noronha, W. Na, T. Sooknoi, D. E. Resasco, *J. Mol. Catal. A: Chem.* **2013**, 388, 47-55.
- [23] J. Lee, Y. Xu, G. W. Huber, *App. Catal. B: Environ.* **2013**, 140-141, 98-107.
- [24] A. J. R. Hensley, Y. Wang, J-S. McEwen, *ACS Catal.* **2015**, 5, 523-536.
- [25] a) D. W. Flaherty, E. Iglesia, *J. Am. Chem. Soc.* **2013**, 135 (49), 18586-18599; b) D. E. Resasco, G. L. Haller, *J. Catal.* **1983**, 82, 279-288.
- [26] a) D. W. Flaherty, A. Uzun, E. Iglesia, *J. Phys. Chem. C* **2015**, 119, 2597-2613; b) D. D. Hibbitts, D. W. Flaherty, E. Iglesia, *J. Phys. Chem. C* **2016**, 120, 8125-8138; c) Flaherty, D. W.; Hibbitts, D. D.; E. Iglesia, *J. Am. Chem. Soc.* **2014**, 136 (27), 9664-9676.
- [27] M. B. Griffin, G. A. Ferguson, D. A. Ruddy, M. J. Bidy, G. T. Beckham, J. A. Schaidle, *ACS Catal.* **2016**, 6, 2715-272.
- [28] P. M. De Souza, R. C. R. Neto, L. E. P. Borges, G. Jacobs, B. H. Davis, D. E. Resasco, F. B. Noronha, *submitted to ACS Catal.* **2016**.

## FULL PAPER

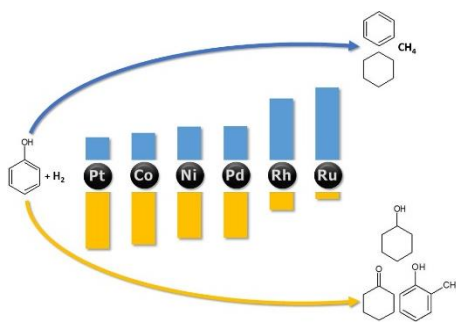
## FULL PAPER

Product distribution as a function of the type of the metal

Author(s), Corresponding Author(s)\*

Page No. – Page No.

Title



WILEY-VCH

Accepted Manuscript